Supplementary Information

From waste plastics to layered porous nitrogen-doped carbon materials with excellent HER performance

Chao Juan, Bing Lan, Chuanchuan Zhao, Hualong Zhang, Dan Li*, Fan Zhang*

Key Laboratory of Green Chemistry and Technology, Ministry of Education, National Engineering Laboratory of Eco-Friendly Polymeric Materials (Sichuan), College of Chemistry, Sichuan University, Chengdu 610065, China

List of Contents

1. Experiment section

1.1 Materials

Polycarbonate (PC) was purchased from Jiangsu Ruijiahong Plastic Co. Magnesium oxide (MgO) was purchased from Chengdu Jinshan Chemical Co. Urea and Potassium hydroxide (KOH) were purchased from Greagent. Nitric acid (HNO_3) was purchased from Chengdu Cologne Chemical Co. Ruthenium (III) Chloride Hydrate ($RuCl_3$ $3H_2O$) was purchased from Adamas. Commercial Pt/C catalyst (20 wt% Pt) was purchased from Tanaka. Commercial Ru/C catalyst (5 wt% Ru) and active carbon (AC) powder were purchased from Macklin. Carbon paper (TGP-H-060) was purchased from Toray. Nafion solution and nafion 117 membrane were purchased from Dupont. High purity N_2 (99.999%) was purchased from Chengdu Changhong Gas Co. All chemical reagents were used as received without further purification.

1.2 Preparation process

Preparation of LPNCS and LPCS

Typically, 0.6 g of polycarbonate, 1.8 g of magnesium oxide, and 0.5 g of urea were evenly mixed and calcined at 1.5 ℃ min^{-1} to 700 ℃ for 1 h in a tubular furnace, then cooled down to room temperature naturally. The mixture was transferred to a beaker with 2 M HNO_3 added and stirred for 24 h at room temperature. After filtration, it was rinsed several times with deionized water and vacuum dried at 60 ℃ for 12 h. LPNCS was collected.

The preparation of LPCS was the same method as LPNCS without adding urea in the procedure.

Preparation of Ru/LPNCS, Ru/LPCS and Ru/AC

100 mg LPNCS was dissolved in 20 mL deionized water, dispersed by ultrasound for 1 h, and stirred for 20 min. Then add 1.5 mL of 26.4 mM ruthenium trichloride ($RuCl_3$) solution to LPNCS solution. The mixture was stirred at room temperature for 6 h, standing for 12 h, and vacuum dried at 60 ℃ for 12 h. Finally, the precursor was calcined at 5 ℃ min^{-1} to 500 ℃ for 3 h in a tubular furnace and naturally cooled down to room temperature.

The preparation of Ru/LPCS and Ru/AC is the same as Ru/LPNCS except using 100mg of LPCS and AC, respectively.

Ru/ LPNCS-optical discs and Ru/ LPNCS-mask replaced PC powder in optical discs and mask, respectively, and the other steps were the same as the synthesis method of Ru/LPNCS

1.3 Characterization methods

Material characterization

The crystal structure of the active metal was determined by Cu target Ka diffraction (λ= 0.15418 nm) and X-ray diffraction (XRD, 6100Lab, Shimazu, Japan) at 40 kV and 30 mA. The scanning angle was 5 ~ 90 ° at the scanning speed of 10 ° min^{-1}. The results were analyzed in Jade 6 software.

The pyrolysis process of polycarbonate was analyzed by Thermogravimetric analysis (TGA, STA 449 F5, NETZSCH, Germany). About 10 mg samples were placed in an alumina crucible and heated to 800 ℃ with 10 ℃ min^{-1} under nitrogen atmosphere.

The surface area and pore size of the carbons and catalysts were determined by the specific surface analyzer (Tristar II 3020, Micromeritics, USA). The samples to be tested were pretreated to degas at 120 ℃ and 300 ℃ for 2 h, respectively, followed by physical adsorption under nitrogen atmosphere at -196 ℃. The results were based on BET equation and BJH method.

Raman spectra were collected by laser Raman spectrometer (XploRA PLUS, HORIBA Scientific, France). The excitation wavelength gratings were 532 nm and 600 gr mm^{-1}, respectively. The Raman displacement was corrected with a silicon wafer before the test.

The elemental chemical states of the catalysts were analyzed by X-ray photoelectron spectroscopy (XPS, AXIS Ultra DLD, Kratos, UK). Al Kα was used as a monochromatic X-ray source. The full spectrum pass energy was 160 eV, and the spectral pass energy was 20 eV. The spectra were corrected by C 1s (284.6 eV).

The actual metal loading was tested by inductively coupled plasma-optical emission spectrometer (ICP-OES, 5100 SVDV, Agilent, USA).

The surface morphology of the catalysts was detected by high-resolution transmission electron microscopy (TEM, Talos F200S G2, Thermo Scientific, USA). A small amount of catalyst is ground, dispersed with anhydrous ethanol, and then dropped directly onto the copper grid. The composition of the catalysts was determined by energy dispersive X-ray spectroscopy (EDS) of model SUPER X.

Electrochemical measurements

Carbon paper and graphite rod were used as working electrode and counter electrode, respectively. Standard Hg/HgO (1 M KOH) was used as the reference electrode in an alkaline solution.5 mg of catalyst powder was added into 0.5 mL of mixed solution (ethanol /Nafion = 5:0.04) and subjected to ultrasonic treatment for 1 h to form uniform catalyst ink (10mg mL^{-1}). The carbon paper (1 cm^2) was coated with 100 μL catalyst ink, and the theoretical loading capacity of the catalyst reached 1 mg cm^{-2}. Then, it was dried at room temperature for 8 h. All potentials were calibrated versus reversible hydrogen electrode (RHE). Electrochemical measurements were performed on an electrochemical workstation (CHI-660E) in a conventional three-

electrode system at room temperature. The working electrodes were activated at a potential of -0.025~0.075 V before testing. The hydrogen evolution reaction (HER) activity was characterized by linear voltammetry scanning (LSV) in 1.0 M KOH solution at a scan rate of 5 mV s^{-1}. All potentials were corrected with 85%-iR to the RHE. The electrochemical active surface area (ECSA) can be estimated by the double-layer capacitance (Cdl), which was measured by cyclic voltammetry (CV) curves which were obtained by setting different sweep speeds (10, 15, 20, 25, 30, 35 mV s^{-1}) in the potential range of 0.05~0.25 V. The current density at 0.15V difference plot was linear with different scan rates. Electrochemical impedance spectroscopy (EIS) was carried out at an overpotential of 13 mV from 10 kHz to 0.1 Hz. The long-term stability test was measured by timing the potential for 10 h at an initial 10 mA cm^{-1} without iR compensation.

2. Material characterization and electrochemical data.

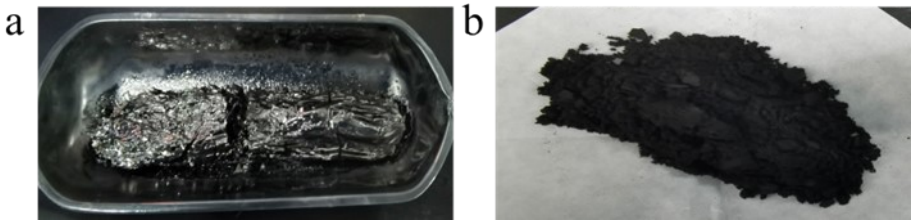

Fig. S1 The material morphology after carbonization in the absence (a) and presence (b) of MgO, respectively.

We found that, in the absence of magnesium oxide, the carbonized plastic agglomerates into a black and hard lump of carbon, as shown in Figure S1a. However, with the addition of MgO, the material transformed into a soft and porous carbon material (Fig. S1b). Therefore, we speculate that MgO can enhance the dispersion of waste plastic powder, which is crucial for forming a more uniform porous material.

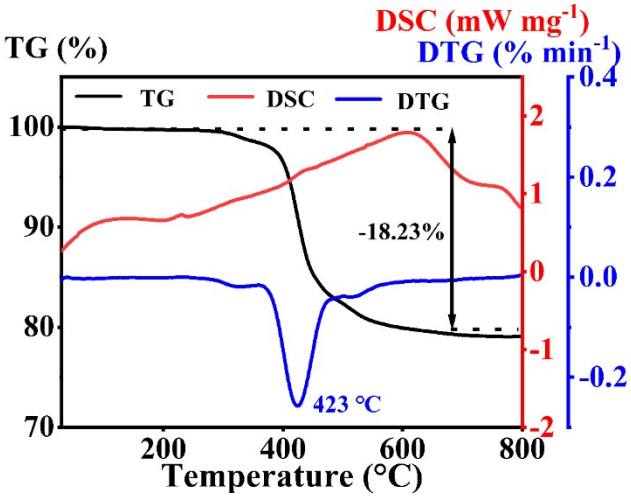

Fig. S2 Isothermal TG (black), DSC (red) and DTG (blue) curves for PC/MgO under Nitrogen gas atmosphere.

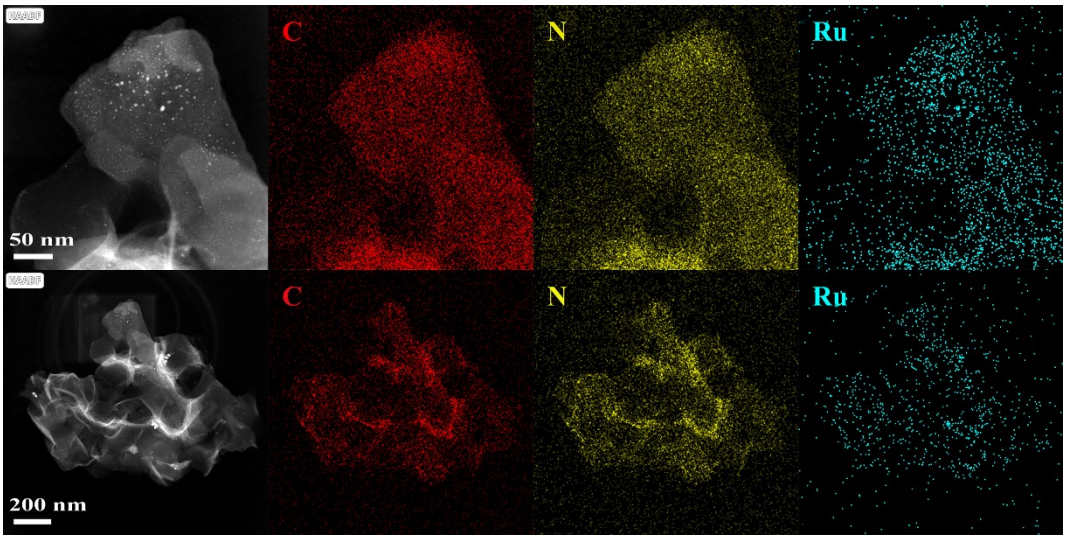

Fig. S3 HAADF-STEM image and the corresponding elemental mapping images of C, N and Ru elements in Ru/LPNCS.

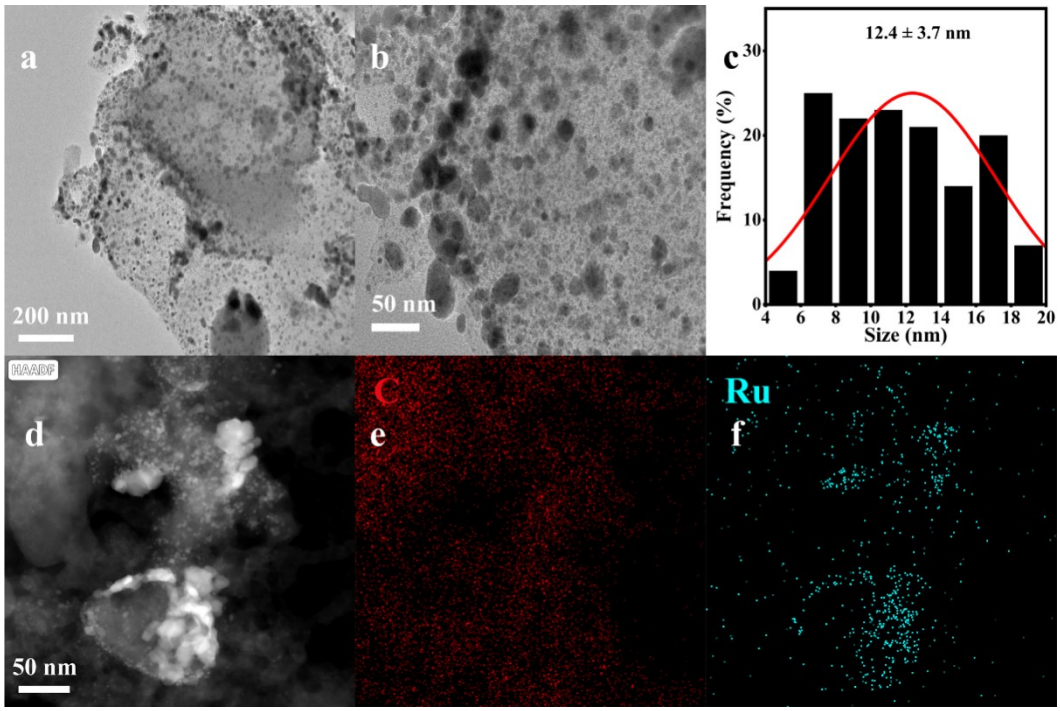

Fig. S4 (a and b) TEM, (c) the size distribution of Ru nanoparticles, (e-f) HAADF-STEM image and the corresponding elemental mapping images of C and Ru elements in Ru/AC.

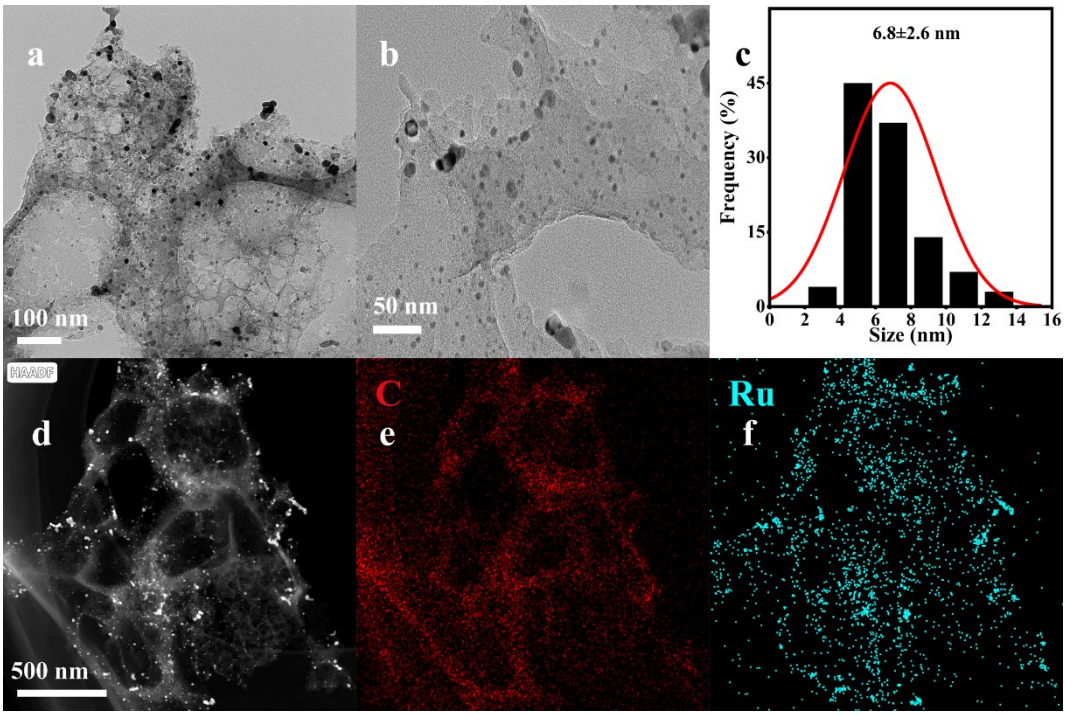

Fig. S5 (a and b) TEM, (c) the size distribution of Ru nanoparticles, (e-f) HAADF-STEM image and the corresponding elemental mapping images of C and Ru elements in Ru/LPCS.

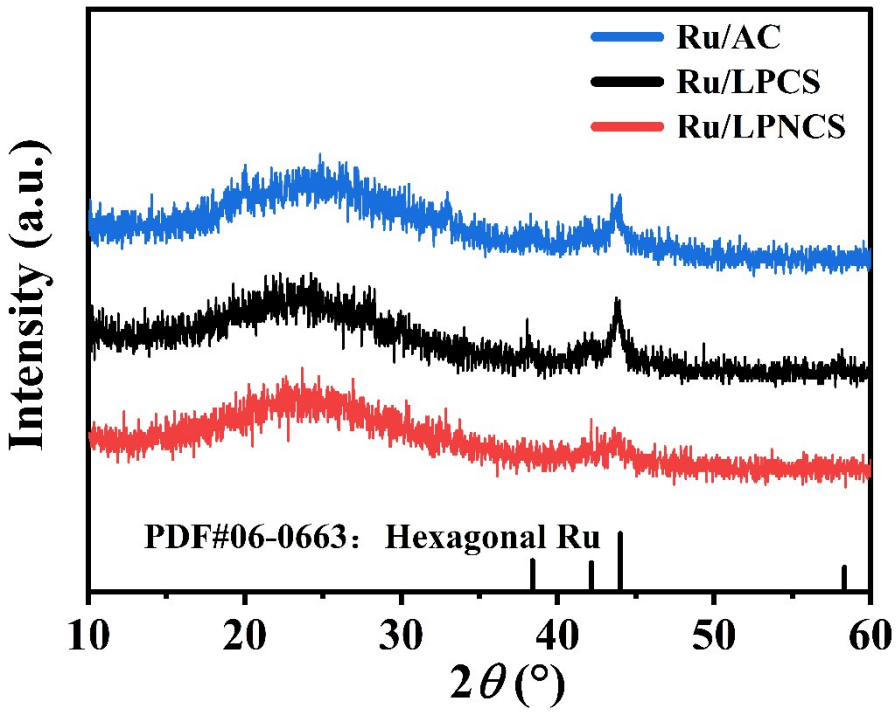

Fig. S6 XRD spectra of Ru/AC, Ru/LPCS and Ru/LPNCS.

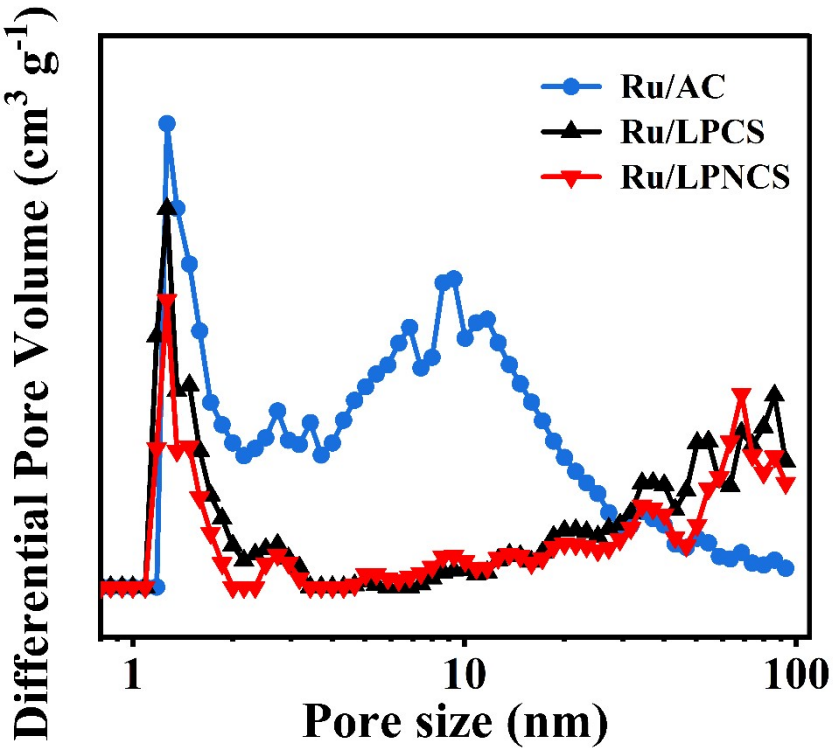

Fig. S7 Pore size distribution of Ru/AC, Ru/LPCS and Ru/LPNCS.

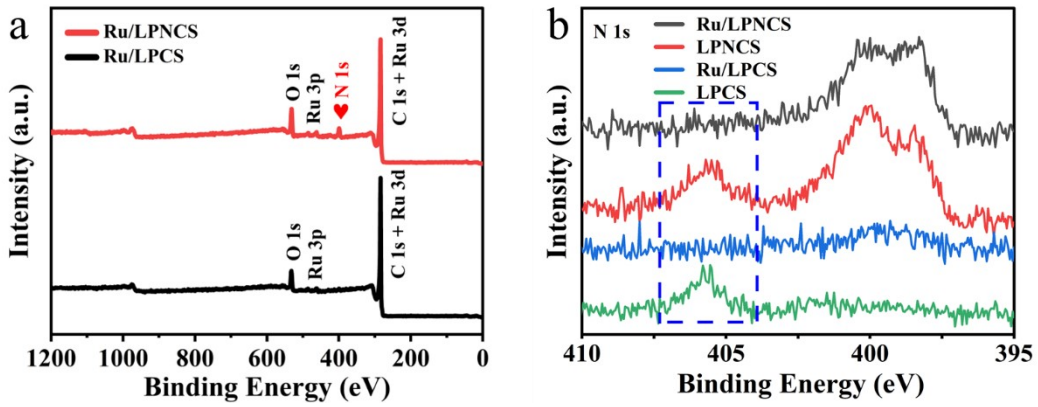

Fig. S8 (a)XPS survey spectrum of the Ru/LPNCS and Ru/LPCS, and (b) N 1s XPS spectra of the LPCS, LPNCS, Ru/LPCS and Ru/LPNCS.

Fig.S8a Ru/LPNCS has a signal of N 1s at 400 eV, indicating that N is successfully incorporated into the carbon material. Fig.S8b Compared to the LPNCS samples, it was found that a small amount of oxidized N species was also present in the N-undoped LPCS. We reasonably speculate that during removing the magnesium oxide template, the oxidized N species may remain on the surface of the LPNCS sample after washing it with nitric acid. However, on the Ru/LPCS and Ru/LPNCS samples, the oxidized N species (405.8 eV) peak is so weak that it is almost unobservable. The possible reason was that these N oxide species were effectively removed from the surface of the samples.

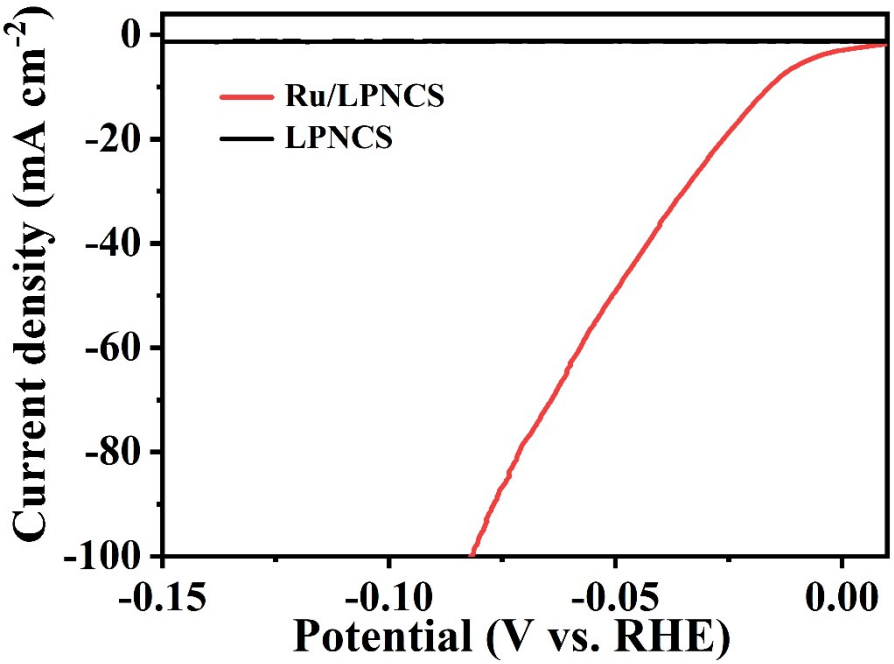

Fig. S9 LSV cures of LPNCS and Ru/LPNC, LPNCS has no HER activity compared with Ru/LPNCS.

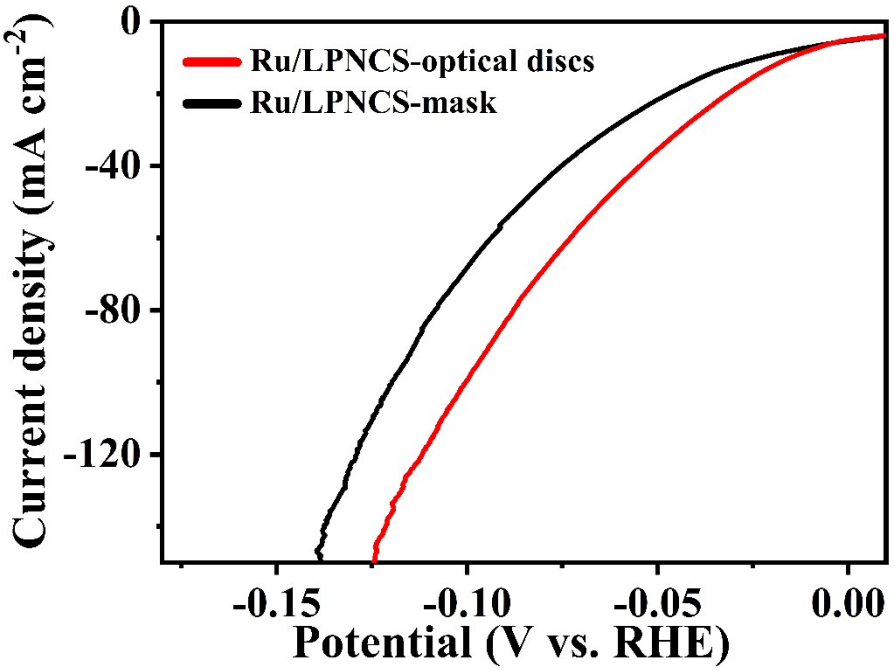

Fig. S10 LSV curves of Ru/LPNCS-optical discs and Ru/LPNCS-mask in 1.0M KOH.

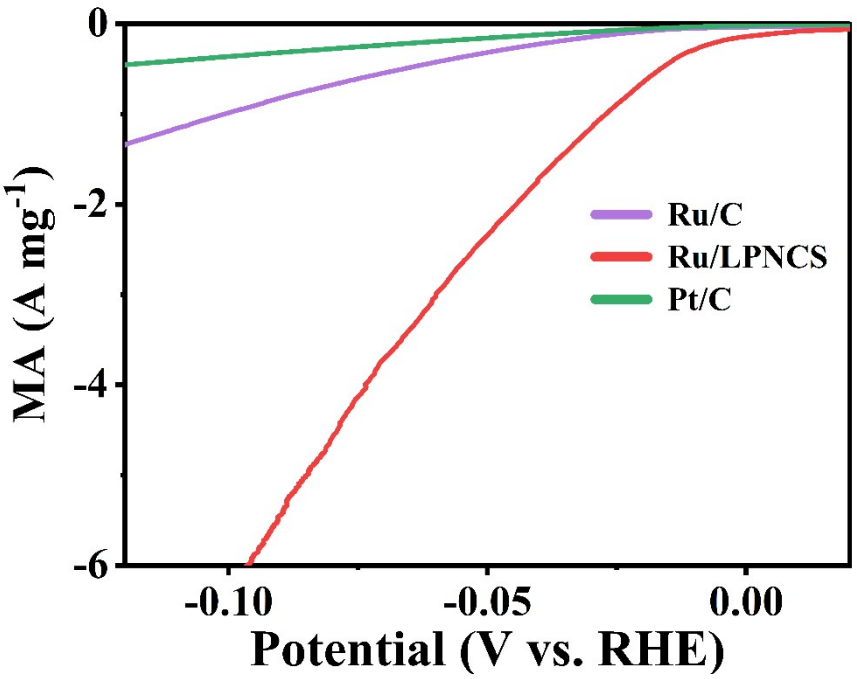

Fig. S11 Mass current density of Ru/C, Ru/LPNCS and Pt/C.

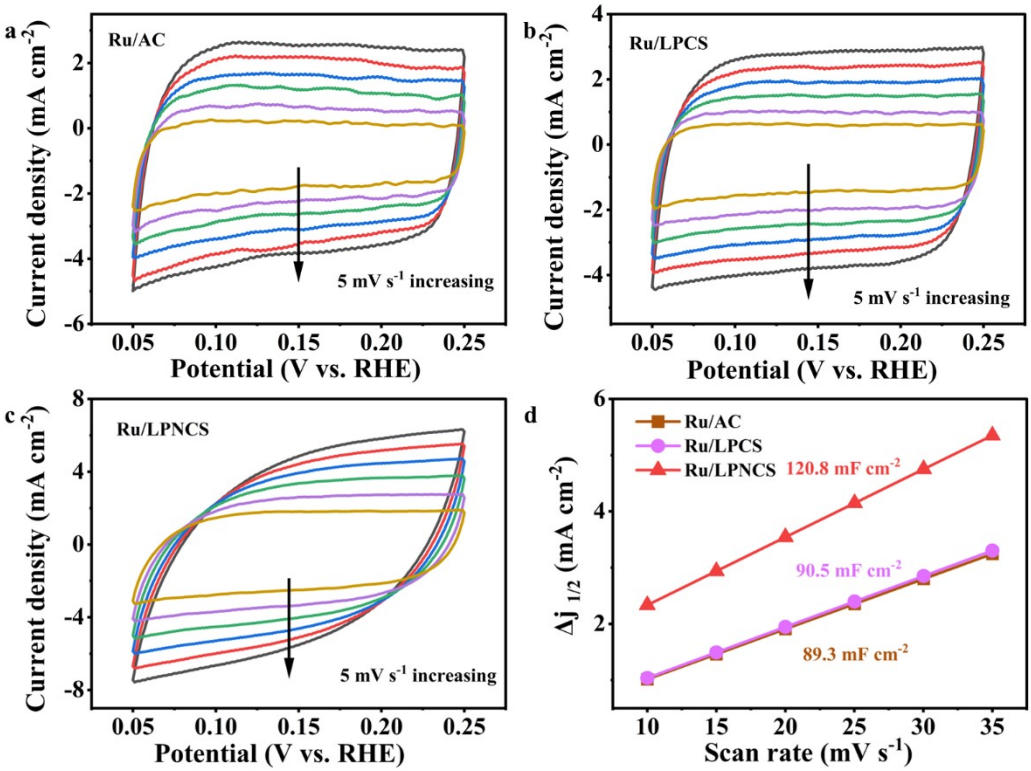

Fig. S12 CV curves of (a) Ru/AC, (b) Ru/LPCS and (c) Ru/LPNCS; (d) Current density as a function of the scan rate for Ru/AC, Ru/LPCS and Ru/LPNCS in 1 M KOH.

Table. S1 Physicochemical properties of LPNCS.

	Specific surface area (m^2 g^{-1})	Pore volume (cm^3 g^{-1})	Pore size (nm)
LPNCS	666.5	0.355	11.1

Table. S2 Results of EDS analysis of Ru/LPNCS.

Z	Element	Mass Fraction (%)
6	C	91.45
7	N	5.85
44	Ru	2.70

Table. S3 Physicochemical properties of catalysis.

	Specific surface area (m^2 g^{-1})	Pore volume (cm^3 g^{-1})	Pore size (nm)
Ru/AC	1023.3	0.569	5.5
Ru/LPCS	868.5	0.368	8.5
Ru/LPNCS	736.3	0.385	8.9

Table. S4 The percentage of different nitrogen species in Ru/LPNCS and LPNCS.

	Pyridinic N	Ru-N	Pyrrolic N	Graphitic N	Oxidized N
Ru/LPNCS	35.3 %	19.6 %	27.8 %	12.2 %	5.1 %
LPNCS	31.7 %	-	40.1 %	7.7 %	20.5 %

- inexistence

Table. S5 Compare the activity of catalysts with different preparation processes or carbon sources

Catalysts	Carbon source	Urea	η_{10}(mV)
Ru/AC	Commercial carbon	Unadded	27
Ru/LPCS	PC powder	Unadded	21
Ru/LPNCS	PC powder	Added	15
Ru/LPNCS-optical discs	Optical discs	Added	15
Ru/LPNCS-mask	Mask	Added	23

Table. S6 Comparison of HER activity of Ru/LPNCS at 1.0 M KOH with other ruthenium-based electrocatalysts in the literature.

Catalysts	Electrolyte solution	η_{10} (mV)	Tafel slope mV dec^{-1}	References
Pt/C	1 M KOH	17	51	This work
Ru/LPNCS	1 M KOH	15	34	This work
RuNi/CQDs	1 M KOH	13	48	1
Ru/OMSNNC	1 M KOH	13	40.41	2
Ru NPs/NC-900	1 M KOH	19	40	3
RuCo@HCSs	1 M KOH	21	32	4
Ru MNSs	1 M KOH	24	33.8	5
RuCo NPs/CNTs	1 M KOH	27	27	6
RuIr@NrC	1 M KOH	28	35	7
P–Ru/C	1 M KOH	31	105	8
NiRu@N–C	1 M KOH	32	64	9
Ru@CN	1 M KOH	32	53	10
ld-Ru@a-Co/Ti	1 M KOH	34	39.6	11
Ru-Mo_2C/CN	1 M KOH	34	80	12
Ru@NCN	1 M KOH	36	37	13
$Ru_{63}Co_{37}$-ANF	1 M KOH	43	42.4	14
RuP_2@NPC	1 M KOH	52	69	15
Ni_5P_4-Ru	1 M KOH	54	52	16
Ru/CoO	1 M KOH	55	70	17
Cu_2-x@Ru NPs	1 M KOH	82	48	18

3. References

1. Y. Liu, X. Li, Q. Zhang, W. Li, Y. Xie, H. Liu, L. Shang, Z. Liu, Z. Chen, L. Gu, Z. Tang, T. Zhang and S. Lu, *Angew. Chem. Int. Ed.*, 2020, **59**, 1718-1726.
2. Y. L. Wu, X. F. Li, Y. S. Wei, Z. M. Fu, W. B. Wei, X. T. Wu, Q. L. Zhu and Q. Xu, *Adv. Mater.*, 2021, **33**, 2006965.
3. Z. Jiang, S. Song, X. Zheng, X. Liang, Z. Li, H. Gu, Z. Li, Y. Wang, S. Liu, W. Chen, D. Wang and Y. Li, *J. Am. Chem. Soc.*, 2022, **144**, 19619-19626.
4. H. Wang, C. Gao, R. Li, Z. Peng, J. Yang, J. Gao, Y. Yang, S. Li, B. Li and Z. Liu, *ACS Sustain. Chem. Eng.*, 2019, **7**, 18744-18752.
5. J. Zhang, X. Mao, S. Wang, L. Liang, M. Cao, L. Wang, G. Li, Y. Xu and X. Huang, *Angew. Chem. Int. Ed.*, 2022, **61**, e202116867.
6. B. Zhang, P. Zhao and T. Wu, *Acs Appl. Energy Mate.*, 2022, **5**, 5633-5643.
7. J. Yu, Y. Dai, X. Wu, Z. Zhang, Q. He, C. Cheng, Z. Wu, Z. Shao and M. Ni, *Chem. Eng. J.*, 2021, **417**, 128105.
8. Y. Zhao, X. Wang, G. Cheng and W. Luo, *ACS Catal.*, 2020, **10**, 11751-11757.
9. Y. Xu, S. Yin, C. Li, K. Deng, H. Xue, X. Li, H. Wang and L. Wang, *J. Mater. Chem. A*, 2018, **6**, 1376-1381.
10. J. Wang, Z. Wei, S. Mao, H. Li and Y. Wang, *Energy Environ. Sci.*, 2018, **11**, 800-806.
11. Z. Ren, M. Tian, N. Cong, H. Jiang, H. Jiang, Z. Xie, J. Han and Y. Zhu, *Chem. Commun.*, 2022,**58**,13588-13591.
12. J. D. Chen, C. H. Chen, Y. Z. Chen, H. Y. Wang, S. J. Mao and Y. Wang, *J. Catal.*, 2020, **392**, 313-321.
13. B. Sarkar, D. Das and K. K. Nanda, *J. Mater. Chem. A*, 2021, **9**, 13958-13966.
14. Y. Wang, Z. Ren, N. Cong, Y. Heng, M. Wang, Z. Wang, Z. Xie, Y. Liu, J. Han and Y. Zhu, *Chem. Commun.*, 2022, **58**, 4631-4634.
15. Z. Pu, I. S. Amiinu, Z. Kou, W. Li and S. Mu, *Angew. Chem. Int. Ed.*, 2017, **56**, 11559-11564.
16. Q. He, D. Tian, H. Jiang, D. Cao, S. Wei, D. Liu, P. Song, Y. Lin and L. Song, *Adv. Mater.*, 2020, **32**, 1906972.
17. J. X. Guo, D. Y. Yan, K. W. Qiu, C. Mu, D. Jiao, J. Mao, H. Wang and T. Ling, *J. Energy Chem.*, 2019, **37**, 143-147.
18. D. Yoon, J. Lee, B. Seo, B. Kim, H. Baik, S. H. Joo and K. Lee, *Small*, 2017, **13**, 1700052.